Journal of Physiology (1993), **470**, *pp.* 211–229
With 13 figures
Printed in Great Britain

CHARACTERIZATION OF THE OUTWARD RECTIFYING POTASSIUM CHANNEL IN A NOVEL MOUSE INTESTINAL SMOOTH MUSCLE CELL PREPARATION

BY ARELES MOLLEMAN, L. THUNEBERG* AND JAN D. HUIZINGA

From the Intestinal Disease Research Unit, Department of Biomedical Sciences, McMaster University, 1200 Main Street West, Hamilton, Ontario, Canada L8N 3Z5

(*Received 20 July 1992*)

SUMMARY

1. The outward rectifying K^+ conductance and underlying single channel behaviour in mouse small intestine (MSI) smooth muscle cells was studied using microelectrode impalement and the patch clamp technique.

2. At 37 °C, smooth muscle cells in MSI explants had a resting membrane potential around −65 mV and showed spontaneous electrical and mechanical activity.

3. Under whole-cell voltage clamp, depolarization of smooth muscle cells in the explants evoked a methoxyverapamil (D600)-sensitive, partially inactivating inward current and a non-inactivating outward current. The outward current was also observed in enzymatically dispersed cells from neonatal mouse small intestine.

4. The reversal potential of the outward current as established in tail current experiments was −70·2 mV. Tail currents could be fitted with a single exponential, suggesting the participation of only one population of channels.

5. The outward current was sensitive to 4-aminopyridine (10^{-4} M), Ba^{2+} (1 mM) and to the presence of Cs^+ in the pipette, but not to D600 (10^{-6} M), or the presence of ATP (1 mM) in the pipette.

6. In the cell-attached patch configuration, a unitary outward current was observed that showed increased activity upon depolarization of the patch. The current–voltage relationship was close to linear with a slope conductance of 186 pS.

7. With normal K^+ (6 mM) in the pipette, the extrapolated reversal potential for the unitary current was around −75 mV, while with high K^+ (120 mM) the reversal potential was close to 0 mV.

8. Averaging single channel traces recorded under a depolarizing pulse protocol resulted in a trace with similar time characteristics as the outward current observed in the whole-cell configuration.

9. The burst behaviour of the channel was described by a simple model consisting of two closed states, C_f (intraburst closed state) and C_s (interburst closed state) and an open state (O). The rate constants in the model showed differential sensitivity to potential changes, channel blockade by Ba^{2+} and equimolar K^+ conditions.

* Visiting Professor from the University of Copenhagen, Anatomy Department, Copenhagen, Denmark.

MS 1631

10. It was concluded that the outward rectifying potassium current in MSI smooth muscle cells is mediated by a 186 pS bursting channel. Voltage dependency and Ba^{2+} blockade are mainly reflected by changes in the transition rate from the open channel state to the interburst closed state.

INTRODUCTION

Outward rectifying potassium currents (I_K) have been observed in most types of excitable cells (Rudy, 1988). They are considered to regulate the rate of the repolarization phase of action potentials (Hille, 1992). Time dependent inactivation is slow or does not occur. I_K-like whole-cell currents have been reported in vascular smooth muscle preparations (rabbit pulmonary artery (Okabe, Kitamura & Kuriyama, 1987); coronary artery (Volk, Matsuda & Shibata, 1991), portal vein (Beech & Bolton, 1989; Lynch, 1985), aorta (Bkaily, Caille, Payet & Peyrow, 1988)), as well as in gastrointestinal preparations (rabbit small intestine (Terada, Kitamura & Kuriyama, 1987), canine colon (Cole & Sanders, 1989) and toad stomach (Walsh & Singer, 1987)). The channels underlying some I_K-like currents have been identified in several preparations such as the giant squid axon (Conti & Neher, 1980) and frog skeletal muscle (Standen, Stanfield & Ward, 1985). In smooth muscle, however, few data on the single channel level are available.

In patch clamp studies it is required that the cell surface is clean and well visible under the microscope. Therefore, smooth muscle patch clamp studies are performed on dispersed cells, freshly used or after a culturing period. However, freshly dispersed cells are likely to be damaged by the enzyme dissociation procedure, while smooth muscle cells in culture are known to 'dedifferentiate' from muscle cells to rapidly proliferating, non-contracting cells (Chamley Campbell, Campbell & Ross, 1979). The explant culturing technique applied in the present study is an alternative that circumvents these problems.

In the present study results from single channel and whole-cell patch clamp recordings are combined to characterize the I_K conductance in mouse small intestinal smooth muscle. Transition rates in a simple kinetic model describing the behaviour of the channel are derived from single channel dwell time distributions, while the effect of voltage, equimolar potassium conditions and Ba^{2+} blockade are expressed in terms of specific changes in these rates.

METHODS

Explant culture

The intestinal tract was taken from neonatal (2–4 day old) CD_1 mice of either sex that were killed by decapitation. A small piece of muscle near the junction of jejunum and ileum was carefully separated from the submucosa and the mesentery and put in culturing medium consisting of M199 (Gibco, Grand Island, NY, USA) supplemented with 2 mM L-glutamine, 4·5 mM $NaHCO_3$, 250 mg/l penicillin and 10% fetal calf serum. Culturing chemicals were obtained from Gibco (Grand Island, NY, USA), except penicillin, which was obtained from Sigma Chemical Co. (St Louis, MO, USA). The muscle was carefully cut under a stereo microscope using a surgical scalpel to pieces of around 0·3 mm^3. The pieces were transferred into a modified Rose chamber, consisting of a bottom coverslip coated with gelatine, a silicone gasket with a round lumen of 1·5 cm in diameter and a height of 1·5 mm and a top coverslip. The chamber pieces were 'glued' together

with Vaseline grease (Fig. 1). In the period before use (10–20 days) the cultures were incubated at 37 °C and fed every 4–5 days through a slit in the silicone gasket. In this period, the explants became attached to the coated bottom coverslip and developed outgrowths of a variety of cell types, sometimes covered by a monolayer of mesothelial cells, which usually deteriorated within

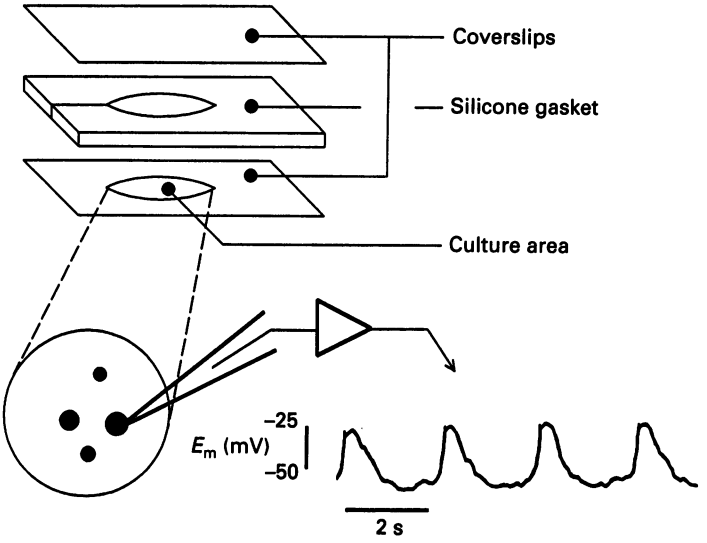

Fig. 1. Modified Rose chamber used in explant culture. The coverslips and gasket are held together by grease. Bottom right: slow wave-like action potentials recorded in the explants.

a week. On the basis of their morphology and contractility (see Results), most cells could be identified as smooth muscle cells, fibroblasts, glial cells supporting neuronal networks, or interstitial cells of Cajal.

Cell dispersion

Enzymatically dispersed cells were obtained using the following procedure. A piece of mouse small intestinal smooth muscle was prepared as described in the previous section. The tissue was minced and put into a dispersion solution consisting of 1 mg ml^{-1} collagenase (Type I, Sigma Chemical Co.), 1 mg ml^{-1} papain (BDH, Toronto, Canada), 2 mg ml^{-1} bovine albumin (Sigma Chemical Co.) and 2 mg ml^{-1} trypsin inhibitor (Type II-S, Sigma Chemical Co.) in Hepes-buffered ECS (extracellular solution; see *Solutions and drugs*) without calcium. The tissue was incubated for 30 min under gentle rotation. This was followed by agitation of the pieces using a small bore Pasteur pipette and washing of the cells by centrifugation ($\pm$1000 r.p.m., 5 min). The cells were plated in M199 culturing medium supplemented as described in the previous section, on gelatin-coated Petri dishes and allowed to adhere for 24 h.

Electrophysiology

Micropipettes made of 1·2 mm, W/Fil glass (WP-Instruments, New Haven, CN, USA) were pulled on a Flaming–Brown puller (Sutter P-80 PC, San Rafael, CA, USA) for both microelectrode and whole-cell patch experiments. The cultures were mounted on a microscope with phase-contrast optics (microelectrode experiments: Nikon, Japan; patch clamp experiments: Zeiss, Germany). Membrane potential measurements were performed using microelectrodes connected through an Ag–AgCl junction to an electrometer (WP-Instruments M-707, New Haven, CN, USA).

Microelectrodes, filled with 3 M KCl, had resistances of 60–100 MΩ. The signals were monitored on a digital oscilloscope (Nicolet 4094, Madison, WI, USA) and stored on a paper writer (Gould 2400S, Cleveland, OH, USA) or on a personal computer (NEC Powermate 386/20, Japan) using a TL-2 interface and Axotape software (Axon Instruments, Foster City, CA, USA). Patch clamp measurements were performed with electrodes (resistance: 2–10 MΩ) connected through an Ag–AgCl junction to the headstage of an Axopatch-1D patch clamp amplifier (Axon Instruments). Voltage clamp control, data storage and analysis were performed on a personal computer (Samsung S550, South Korea) using a TL-1 interface and pCLAMP software (Axon Instruments). Signals were monitored on a digital oscilloscope (Nicolet 3091). In both microelectrode and whole-cell patch clamp experiments, the micropipettes were mounted on hydraulic micromanipulators (Narashige MO-303, Japan) to approach the cells. Temperature was maintained at 36·5±0·5 °C using a Zeiss heating stage (in the patch clamp experiments) or a heating lamp (in the microelectrode experiments), in combination with a heating coil wound around a glass capillary to preheat the superfusion solutions. In the microelectrode experiments the cell membrane was penetrated using a Piezo step motor (PM 10, Stoelting, Chicago, IL, USA).

Whole-cell patch clamp

In the patch clamp experiments a gigaseal (cell-attached patch configuration) was formed by application of gentle suction. Approximate liquid junction potentials (LJPs) were calculated using the Henderson liquid junction potential equation (Barry & Lynch, 1991), where ion activities were represented by concentrations. Pipette potentials were adjusted to these potentials. The largest calculated LJP (3·9 mV) was found between standard ECS and standard ICS (intracellular solution; see *Solutions and drugs*). The whole-cell patch clamp configuration was established by disrupting the membrane under the pipette, either by large current injection ('zapping'), or by a suction pulse. In the whole-cell experiments, capacitive transients were cancelled as well as possibly using the amplifier's compensation circuitry. The access resistance of around 20 MΩ, forming a resistance–capacitance (RC) circuit with the cell capacity with a τ (time constant) of 0·8 ms and causing a voltage drop of around 4% over the cell resistance, was compensated for not more than 50% to prevent excessive noise and oscillation. Resting current was set to zero at the start of each experiment. An 80 dB/decade low-pass filter was applied at a cut-off frequency (−3 dB) of 2 kHz or higher. The sampling rate was 5 kHz. Passive current components were removed where mentioned, using positive–negative (P/N) subtraction. Passive current components were recorded by application of a voltage protocol in a membrane potential range where no active conductances were activated (−60 to −80 mV). These traces (4 or 5) were added, scaled and subtracted from the actual current tracing, leaving only the active current component.

Single channel recording

Single channel activity was recorded in the cell-attached patch and the outside-out excised patch configuration. Outside-out excised patches were obtained by gently pulling the patch pipette away from the cell after establishment of the whole-cell configuration. Single channel recordings were filtered on-line (2 kHz cut-off frequency, −3 dB low pass) and sampled at 5 or 10 kHz. The recordings were idealized automatically if the signal-to-noise ratio was better than around five (most of the data), using a single threshold at half the channel amplitude. With noisier data (the smallest amplitude point in each *I–V* relationship, see Fig. 8) the same procedure was followed but with manual control over each transition. Idealized data was analysed using the pSTAT module of the pCLAMP patch clamp software package (Axon Instruments). In the time distribution analysis, events shorter than 0·5 ms were ignored to prevent filtering and sampling artifacts. Bin widths were manually adjusted from a default value of 1/400 of the time range.

All results are presented as means±S.E.M. (n = number of experiments).

Solutions and drugs

The cells were superfused with one of two types of 'extracellular solution' (ECS), using different buffers. Composition of the carbonate-buffered ECS ('Krebs') used in microelectrode experiments (mM): NaCl, 120; NaH_2PO_4, 1·2; $MgCl_2$, 1·2; $CaCl_2$, 2·5; KCl, 5·9; D-glucose, 11·5; $NaHCO_3$, 20·2; pH set at 7·4 using 95% O_2–5% CO_2 gas. Composition of Hepes-buffered ECS (Molleman, Nelemans & Den Hertog, 1989) used in patch clamp experiments (mM): NaCl, 125; KCl, 6; $MgCl_2$, 2·5; $CaCl_2$, 1·2; NaH_2PO_4, 1·2; Hepes, 10; D-glucose, 11; pH set at 7·4 with NaOH. This solution

was also used in the standard cell-attached patch experiments. Patch pipettes in 'equimolar conditions' experiments (in cell-attached patch mode), in whole-cell or in outside-out excised patch mode were filled with 'intracellular solution' (ICS) with the following composition (mM): KCl, 126; NaCl, 5; $MgCl_2$, 1·2; Hepes (Boehringer, FRG), 10; D-glucose, 11; pH set at 7·2 with KOH. The free calcium concentration in the ICS was calculated using a computer iteration method similar to the one applied by Fabiato & Fabiato (1979). Mostly 0·1 mM EGTA and 48 μM $CaCl_2$ were used to obtain a free calcium concentration of around 150 nM.

Salts were obtained from BDH Inc. (Toronto, ON, Canada) unless otherwise stated. Disodium adenosine triphosphate, D600 (methoxyverapamil hydrochloride), 4-aminopyridine and diltiazem hydrochloride, all water soluble, were obtained from Sigma Chemical Co.

RESULTS

Functionality of the smooth muscle cells in the explants

When taken from the abdomen of neonatal mice, the whole small intestine showed rhythmic contractions with a frequency of 24–48 contractions per min, propagating along the longitudinal axis of the intestine. Isolation and cutting of the muscle layer did not stop these contractions, nor did attachment (after 2–5 days) to the bottom of the modified Rose chamber (see Methods). After 5–10 days cells of different types had grown out of the explant (Table 1). The type of cells within the explant centre could not be determined visually since that area of the culture was many cell layers thick.

The smooth muscle cells in the explant had a resting membrane potential of $-53{\cdot}0 \pm 1{\cdot}2$ mV ($n = 26$), as measured with microelectrodes in Krebs physiological salt solution. The cells displayed slow wave-like spontaneous rhythmical depolarizations (Fig. 1), that coincided with contractions of the explants. The contractions and depolarizations were completely abolished in the presence of D600 (10^{-6} M, $n = 7$). Compared to the whole intestine, the frequency of the contractions was slightly lower in culture ($23{\cdot}2 \pm 0{\cdot}7$ contractions per min, $n = 24$).

Macrocurrent characteristics of smooth muscle cells

Cells were selected for whole-cell patch clamp experiments on the basis of their morphology (see previous section) and their location in the outgrowths of the explant, since cells inside the explant were highly coupled to neighbouring cells, impairing an adequate voltage clamp. In the whole-cell patch clamp configuration an ensemble of voltage pulses ranging from -100 to $+150$ mV membrane potential was applied to cells clamped at -60 mV holding potential to detect voltage-dependent currents. No active currents were detected at potentials more negative than -40 mV. Depolarizing voltage pulses of incrementing amplitude from a holding potential of -60 mV, evoked current responses consisting of an initial inward current, which showed partial time-dependent inactivation, followed by a non-inactivating outward current (Fig. 2). Only inward current was present when potassium in the pipette solution was substituted by caesium (Fig. 3*A*). The extrapolated reversal potential derived from the linear part of the current–voltage relationship (Fig. 3*B*) was 60 mV. The inward current was completely abolished by the blockers of voltage-dependent calcium channels, diltiazem (10^{-5} M, $n = 4$), or D600 (10^{-6} M, $n = 9$).

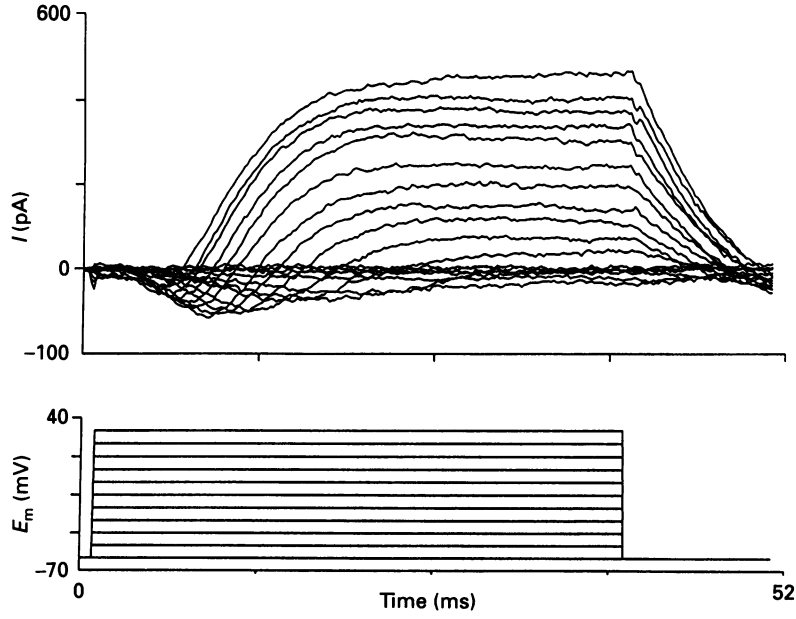

Fig. 2. Whole-cell current ensemble with normal ECS and ICS. Holding potential was −60 mV. Current responses to 11 voltage steps with increments of 10 mV are superimposed. Passive current components were removed by P/N subtraction. Pulse intervals were 200 ms within the P/N protocol and 3 s between protocols. Upward deflection denotes outward current.

TABLE 1. Morphology of cells in mouse small intestine explant cultures

Cell type	Appearance in phase-contrast microscopy
Smooth muscle cell	Contracting rhythmically, spindle-shaped, arranged in bundles
Glial cell	Flattened cell supporting dark, thin axon bundles
Mesothelial cell	Flat, tile-shaped cell, arranged in a closed monolayer
Macrophage	Isolated, round cell with veil-like extremities
Interstitial cell of Cajal	Dark cell with 2–4 processes and a large nucleus, often located on top of a bundle of smooth muscle cells
Other cells	Cells which do not match any of the above, most of them are likely to be fibroblasts

The following experiments were performed in the presence of diltiazem (10^{-5} M) or D600 (10^{-6} M) to block calcium inward current and to decrease contribution of calcium-dependent potassium current. An outward current was present in response to membrane depolarizations under these circumstances in smooth muscle cells of the explants, as well as in dispersed cells. The current activated with a delay of 1–2 ms from the onset of the test pulse, while time-dependent inactivation was not detected within 500 ms (Fig. 4*A*). These characteristics did not vary significantly between explant cells and dispersed cells. The *I–V* relationship for the outward current showed conductance activation in the membrane potential range of −35 to 20 mV

(Fig. 4*B*). The tails could be fitted well with a single exponential, suggesting the contribution of only one conductance to the outward current under these conditions. The reversal potential for the outward current was determined in after-pulse experiments (Fig. 5) and it was found that reversal occurred at $-70{\cdot}2 \pm 3{\cdot}4$ mV ($n = 6$), close to the potassium equilibrium potential (-76 mV).

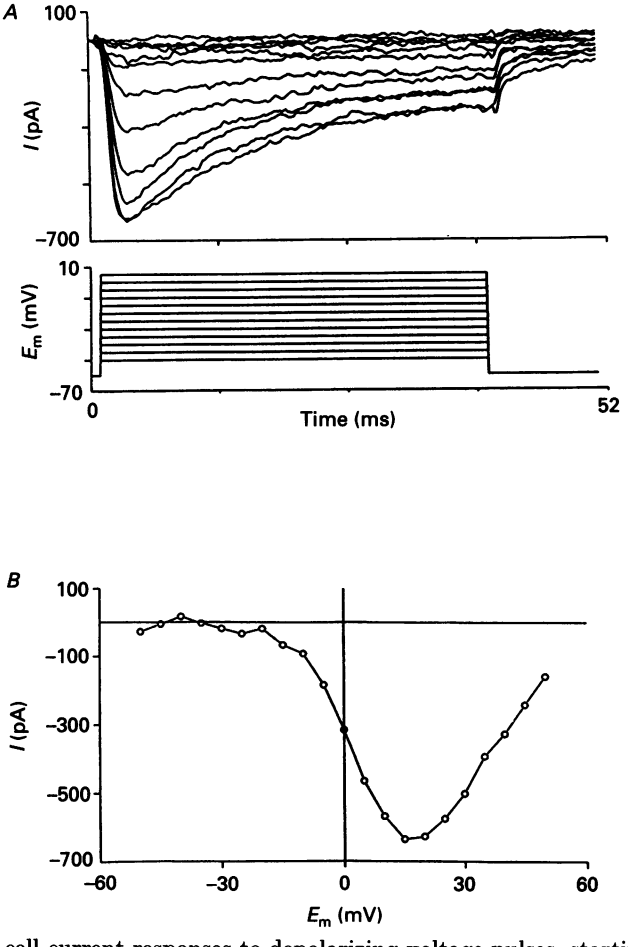

Fig. 3. Whole-cell current responses to depolarizing voltage pulses, starting at -50 mV with 5 mV increments, with normal ECS but K^+ in the ICS replaced by Cs^+. Holding potential was -60 mV. *A*, current responses to the first 12 voltage steps are displayed. Further depolarization showed decreasing inward currents. Passive current components were removed by P/N subtraction. Pulse intervals were 200 ms within the P/N protocol and 3 s between protocols. Downward deflection denotes inward current. *B*, current–voltage relationship. Current is measured as peak inward current.

The outward current as evoked by a test pulse to 0 mV was partially blocked by 4-aminopyridine (10^{-4} M, in two observations 70 and 73% block) and barium ions (1 mM, 42 ± 11% block, $n = 3$, Fig. 6). Sensitivity of the outward current to

intracellular ATP was tested by application of 1 mM ATP in the patch pipette; the outward current amplitude to a test pulse to +10 mV under these conditions was 630±150 pA ($n = 10$), while this value was 594±210 pA ($n = 8$) in the absence of ATP.

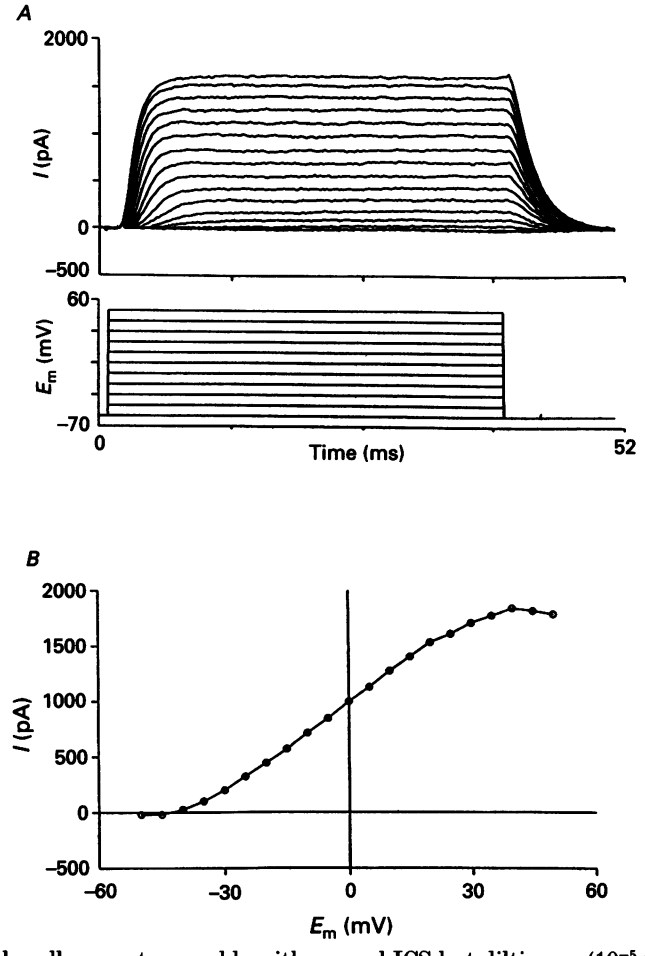

Fig. 4. Whole-cell current ensemble with normal ICS but diltiazem (10^{-5} M) added to the ECS. Holding potential was −60 mV. *A*, current responses to membrane depolarizations with increments of 5 mV. Passive current components were removed by P/N subtraction. Pulse intervals were 200 ms within the P/N protocol and 3·5 s between each protocol. Upward deflection denotes outward current. *B*, current–voltage relationship. Current is measured as steady-state outward current.

Single channel recording of outward rectifying channels

Detection of a bursting outward channel

In the cell-attached patch configuration, an outward unitary current was observed which showed increased opening upon membrane depolarization (more negative pipette potentials). The channel was present in about 25% of the patches in the explants ($n = 25$) and dispersed cells ($n = 5$). Each experimental condition described

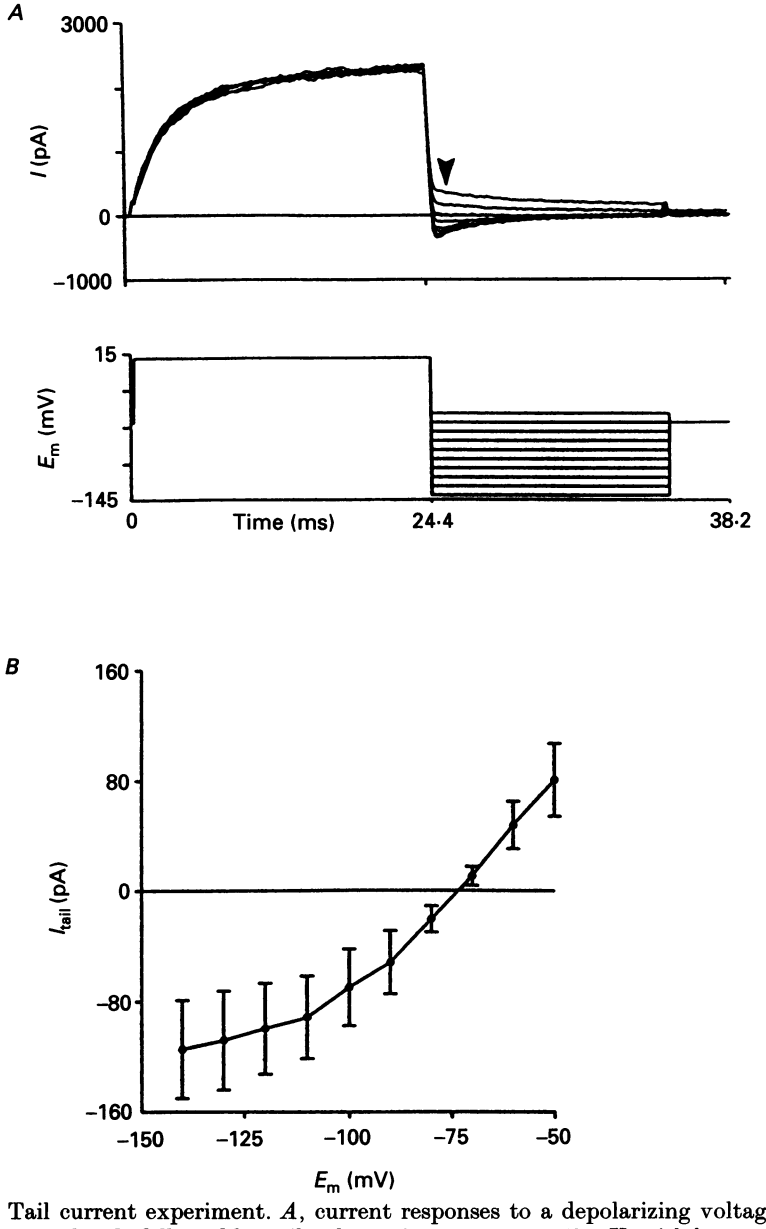

Fig. 5. Tail current experiment. *A*, current responses to a depolarizing voltage step of constant amplitude followed by tail pulses (10 ×, start at −50 mV, with hyperpolarizing increments of 10 mV). Holding potential was −60 mV. Pulse interval was 1000 ms. Traces are displayed in split time. Upward deflection denotes outward current. *B*, relationship between the amplitude of the tail pulses and the tail currents ($n = 6$). Tail current is measured typically as current at the time indicated by the arrowhead in *A*, minus the resting current at that potential.

hereafter is represented by a complete data set, obtained from a single patch for each experimental condition. Additional partial data sets recorded from the other patches were consistent with the described findings. The channel gating was burst-like

(Fig. 7), with rapid openings and closures, intermittant with silent periods. The I–V relationship for the unitary current had a slope conductance of 186 ± 18 pS ($n = 13$) (Fig. 8). The extrapolated reversal pipette potential was 10 mV. Assuming a resting membrane potential of -65 mV, the reversal potential would be -75 mV. The

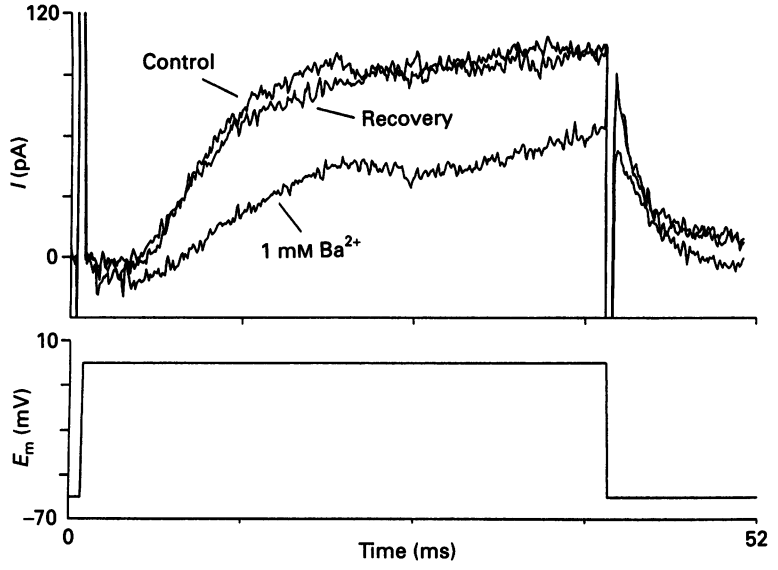

Fig. 6. Effect of 1 mM Ba^{2+} on the outward current. Current peaks at the start and the end of the test pulse are capacitive. Traces represent typical steady-state current responses to test pulses to 0 mV. Holding potential was -60 mV. Pulse intervals were 3 min. Upward deflection denotes outward current.

steady-state open probability (P_{open}) at each potential was determined by fitting amplitude distributions with two Gaussian functions, G_{open} and G_{closed}, so that

$$P_{open} = \frac{\int G_{open}}{\int G_{closed} + \int G_{open}}.$$

Figure 9 shows that the open probability increases dramatically upon membrane depolarization.

Relation to whole-cell outward current

The relationship of the single channel to the whole-cell outward current was investigated in two ways. Firstly, an averaging experiment was performed to compare the time course of the whole-cell outward current to an averaged single channel current response. The averaged current possessed a time course similar to the whole-cell outward current evoked by a test pulse to 0 mV (Fig. 10): τ_{act} for the average current was 7·2 ms, while the step to 0 mV in the whole-cell protocol evoked a current with τ_{act} of 6·9 ms. Secondly, channel blockers that were shown to be effective in inhibiting whole-cell currents were applied to outside-out excised patches. Single channel gating but not unitary current was reversibly inhibited by barium ions (1 mM, $n = 2$) and 4-aminopyridine (10^{-4} M, $n = 2$).

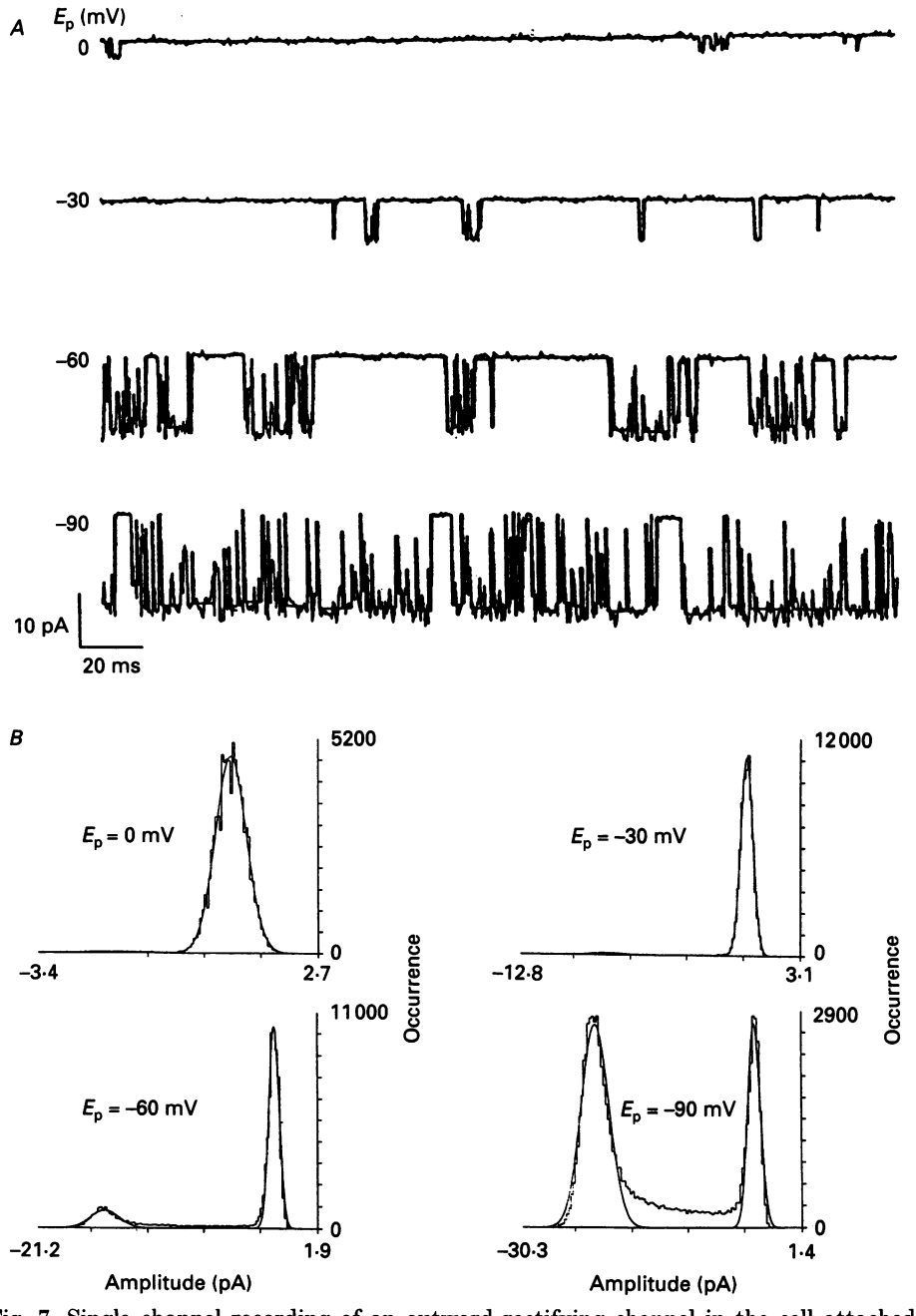

Fig. 7. Single channel recording of an outward rectifying channel in the cell attached patch configuration at different pipette potentials. Note that negative pipette potentials result in membrane depolarization. The pipette contained normal ECS. *A*, samples of channel activity with idealized traces superimposed. Downward deflection denotes outward current. Channel activity was recorded for 30 s at each potential. *B*, All-point amplitude histograms for the single channel recordings of *A*, with the results of double Gaussian fits superimposed. The right-hand curves of each graph represent the closed state, while the left-hand curves represent the open state of the channel.

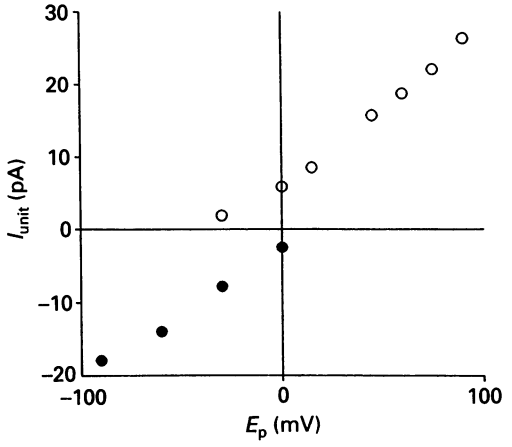

Fig. 8. Single channel current–voltage relationship (cell-attached patch). ●, pipette containing normal ECS. ○, pipette containing equimolar K^+ solution. Note that negative pipette potentials result in membrane depolarization.

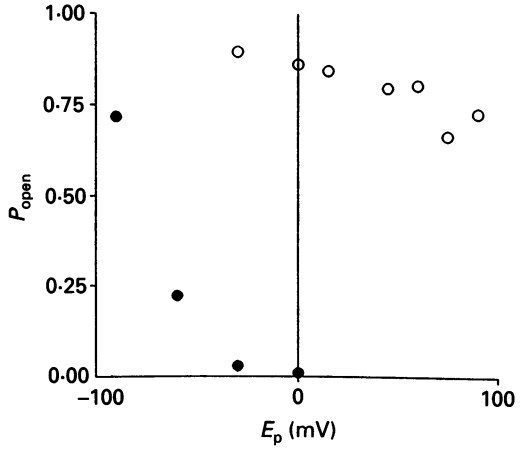

Fig. 9. Single channel open probability (cell-attached patch). ●, pipette containing normal ECS. ○, pipette containing equimolar K^+ solution. Note that negative pipette potentials result in membrane depolarization.

Determination of kinetic parameters

One minute recordings were made of channel activity at different potentials in patches that did not show double openings. The recordings were transformed to sets of open and closed times manually, or by computer if the signal:noise ratio and baseline stability allowed this. Open and closed time distributions, derived from these tracings, were fitted with one or multiple exponentials (Fig. 11). It was found that the open time distributions could be fitted optimally with a single fast exponential, while the closed time distributions could be fitted optimally with two exponentials, one fast and one relatively slow. The exponential functions obtained as a result of the fitting procedures were used to calculate the rate constants for the

simplest model for a bursting channel at a given potential (Colquhoun & Sigworth, 1983; Garcia Diaz, 1991). The model has three states, an open state (O), an intraburst 'fast' closed state (C_f) and an interburst 'slow' closed state (C_s):

$$C_f \underset{r_{C_fO}}{\overset{r_{OC_f}}{\rightleftharpoons}} O \underset{r_{OC_s}}{\overset{r_{C_sO}}{\rightleftharpoons}} C_s,$$

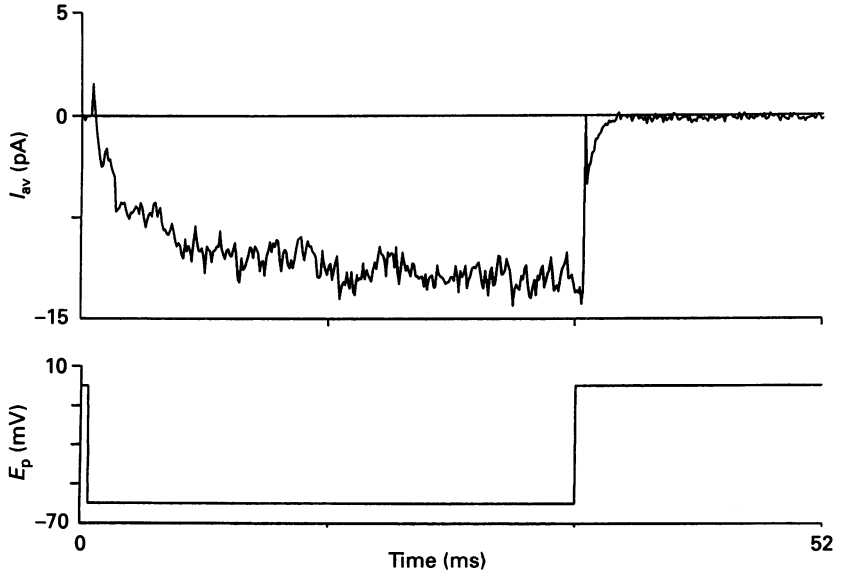

Fig. 10. Averaged traces of 64 single channel current responses to a depolarizing voltage pulse (pipette potential from 0 to −60 mV). Downward deflection denotes outward current.

where r represents the transition rates. The dwell time distribution for the open state follows the equation

$$f(t) = \alpha \exp(-\alpha t) \quad (t \geqslant 0),$$

with $\alpha = r_{OC_f} + r_{OC_s} = 1/\tau$. The dwell time distribution for the closed state follows

$$f(t) = \left(\frac{r_{OC_f}}{r_{OC_f} + r_{OC_s}}\right) r_{C_fO} \exp(-r_{C_fO}) + \left(\frac{r_{OC_s}}{r_{OC_f} + r_{OC_s}}\right) r_{C_sO} \exp(-r_{C_sO}) \quad (t \geqslant 0),$$

wherein $r_{C_fO} = 1/\tau_{fast}$ and $r_{C_sO} = 1/\tau_{slow}$. The transition rates were calculated from the fitting results using these relations. Figure 12 shows the voltage dependency of the transition rates under normal conditions. All transition rates show some degree of voltage dependency, with r_{OC_s} being affected most dramatically, resulting in a decrease of interburst closed state occurrence upon membrane depolarization.

Modification of kinetic parameters under equimolar K^+ conditions and by application of barium ions

When the patch pipette was filled with salt solution resembling the intracellular ionic composition (ICS), the extrapolated reversal potential shifted 65 mV, following the shift in potassium equilibrium potential, while the slope conductance remained

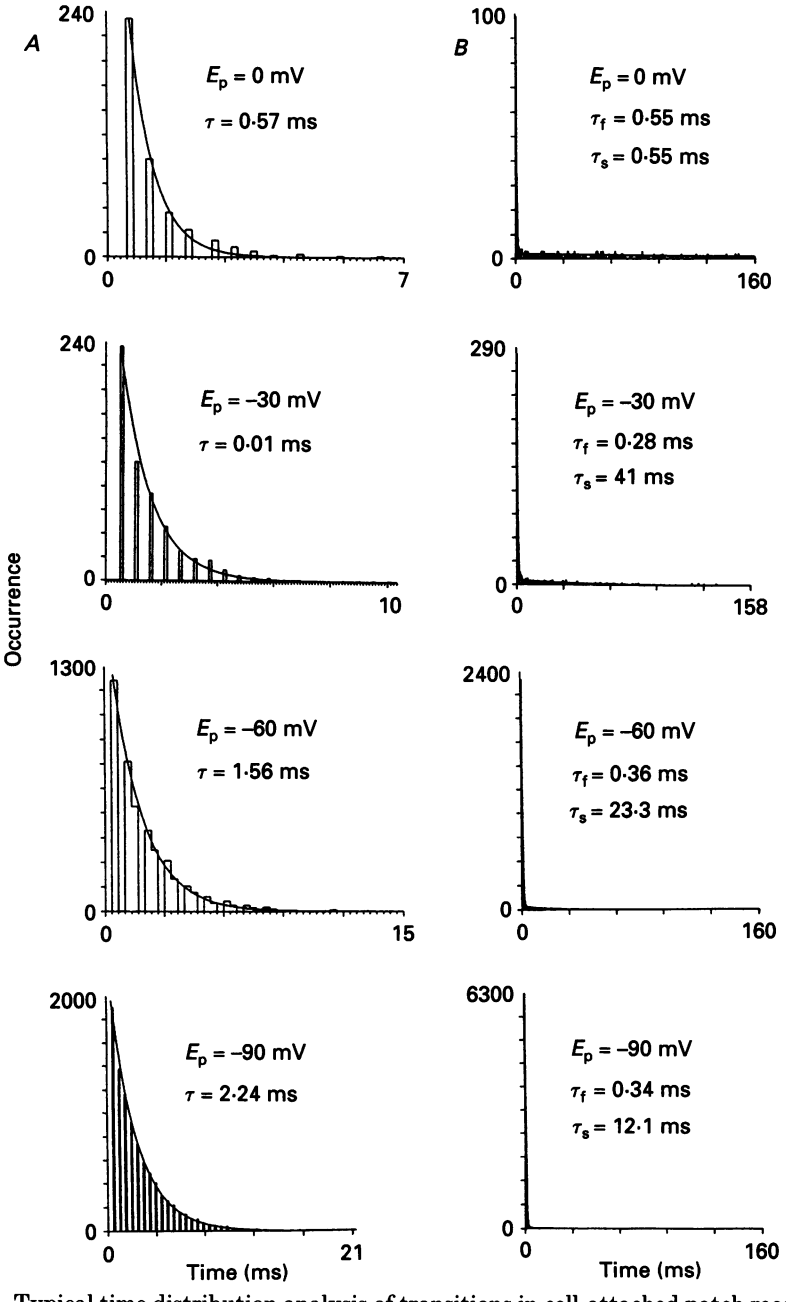

Fig. 11. Typical time distribution analysis of transitions in cell-attached patch recordings at different potentials. The pipette contained normal ECS. See text for the calculation of transition rates from the fitting results. *A*, open state dwell time distributions fitted with a single exponential. *B*, closed state dwell time distributions fitted with two exponentials.

constant (Fig. 8). The voltage dependency of the open probability under these conditions was markedly reduced (Fig. 9). Application of the above kinetic analysis to the data acquired under equimolar K^+ conditions showed that the transition rates

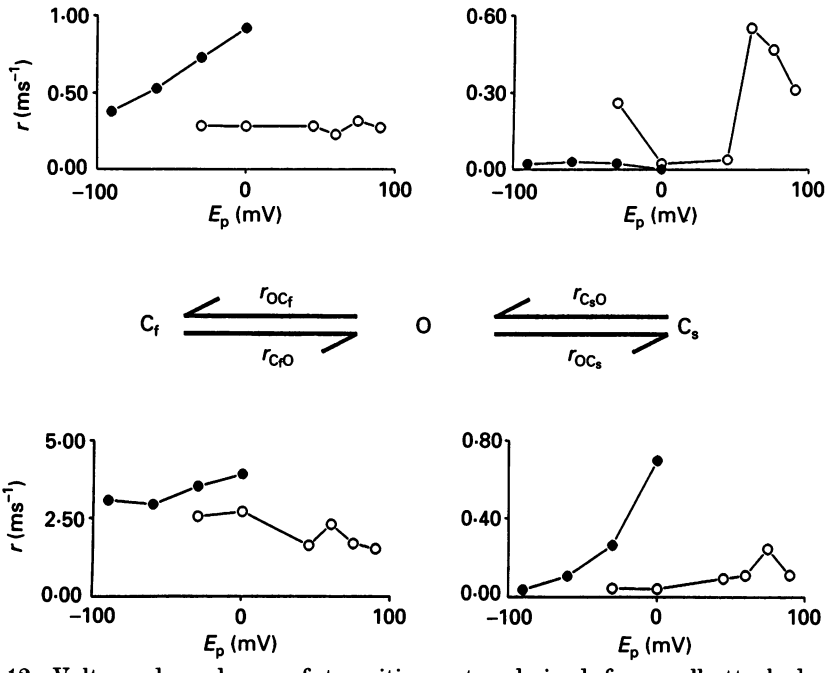

Fig. 12. Voltage dependency of transition rates derived from cell-attached patch recordings. ●, pipette containing normal ECS. ○, pipette containing equimolar K^+ solution. Note that negative pipette potentials result in membrane depolarization.

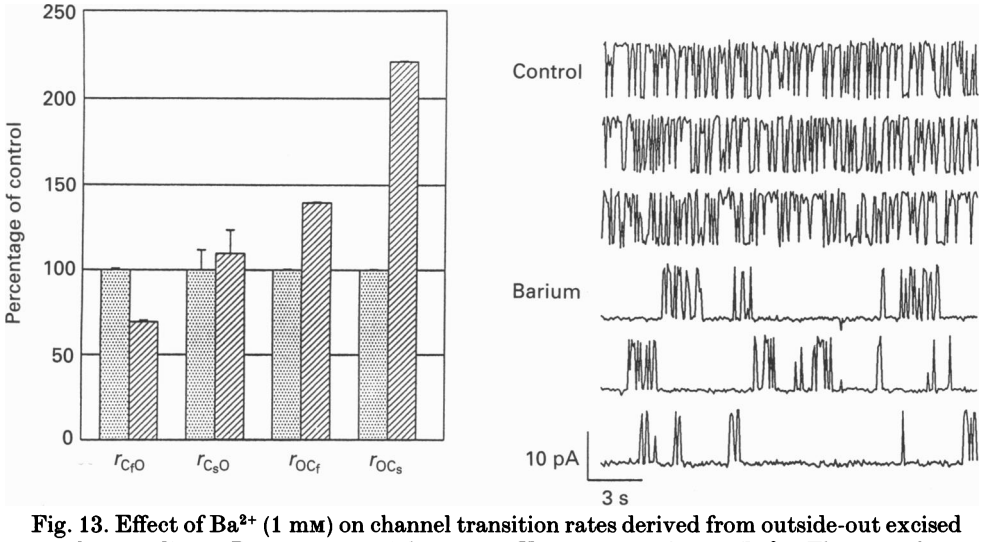

Fig. 13. Effect of Ba^{2+} (1 mM) on channel transition rates derived from outside-out excised patch recordings. Pipette potential was 0 mV; ▨, control; ▨, Ba^{2+}. The top three (continuous) traces represent control activity, the bottom (continuous) traces represent activity in the presence of Ba^{2+}. Note that the time scale is compressed. Upward deflection denotes outward current.

between the open and the intraburst closed state lost their voltage sensitivity, while the other two transition rates became more erratic (Fig. 12). In outside-out excised patches, extracellular Ba^{2+} (1 mM) did not affect the unitary current amplitude, but decreased the open probability of the channel. Determination of the transition rates under these conditions showed that the r_{OC_s} transition rate was affected most significantly (Fig. 13).

DISCUSSION

The results show the presence of at least two currents in smooth muscle cells of mouse small intestine explants; an inward current sensitive to L-type calcium channel blockers and an outward rectifying current. The latter was also studied in dispersed cells of the same tissue. The main charge carrier of the outward current is potassium, because the reversal potential as revealed in tail current experiments was very close to the potassium equilibrium potential and the current could not be evoked when intracellular potassium was substituted by the potassium channel blocker caesium. The current is not the strongly calcium-dependent potassium current omnipresent in smooth muscle cells (Latorre, Oberhauser, Labarca & Alvarez, 1989), because it was not affected by conditions where the intracellular free calcium concentration was buffered by EGTA and calcium influx was blocked by calcium antagonists. It was also shown that the current was not inhibited by intracellular ATP, which excludes another group of potassium channels, the so called $I_{K,ATP}$ channels, well described in pancreatic β-cells and cardiac cells (Ashcroft, 1988) and likely present in certain types of smooth muscle (Nelson, Patlak, Worley & Standen, 1990). The observed current shares gross characteristics with the neuronal and muscular delayed outward rectifying current: it is highly selective for potassium, it clearly has a delay from potential change to onset of the current, it is slowly or not inactivating and it is sensitive to 4-aminopyridine and barium ions (Hille, 1992). Whole-cell currents with these characteristics have been observed in all major groups of smooth muscle preparations, such as vascular smooth muscle (Volk *et al.* 1991; Okabe *et al.* 1987), gastrointestinal smooth muscle (Terada *et al.* 1987; Cole & Sanders, 1989) and in smooth muscle cell lines (Molleman, Nelemans, Van Den Akker, Duin & Den Hertog,1991).

Patch clamp studies on smooth muscle are usually performed on fresh enzymatically dispersed cells, although most workers recognize the possibility of alteration or destruction of membrane structures in the dissociation process. This risk is taken because the alternative, allowing the cells to recover in (primary) culture for several days, is known to often alter the cell properties dramatically. The changes can be summarized as 'dedifferentiation' and include loss of contractility and certain receptor mediated responses (Chamley Campbell *et al.* 1979). It was proposed that platelet-derived growth factor and related substances in the serum induce this reaction, which is consistent with the observation that removal of serum from the culturing medium can sometimes reverse dedifferentiation (Tagami *et al.* 1986). The explant culturing technique used in the present study provides the possibility to obtain smooth muscle cells that are not treated with enzymes and have not lost their function. The explants retain a highly stable spontaneous activity in culture, despite their exposure to serum-supplemented medium. This suggests that in mouse small

intestine conservation of some degree of tissue integrity inhibits smooth muscle dedifferentiation.

The use of the explant culturing technique in the present study provides a control for the results obtained from dispersed cells, removing a previously intrinsic uncertainty in interpretation of the latter. It was found that the outward rectifying potassium current in dispersed cells is not different from the current found in smooth muscle cells in the explants. Hence, the enzyme treatment has not altered the I_K characteristics in this preparation.

In the cell-attached patch configuration, a 186 pS channel with an extrapolated reversal potential around −75 mV was identified, suggesting potassium as the main charge carrier. The shift in *I–V* relationship as a result of equimolar potassium conditions was consistent with this. The channel is likely to underlie the outward rectifying current described above, because the time course of averaged pulse responses and sensitivity to blockers matched the macrocurrent characteristics. The channel seems distinct from the I_K channel in rabbit jejunum, which has a low to medium unitary conductance and relatively slow gating (Benham & Bolton, 1983). The I_K channels in giant squid axons (Conti & Neher, 1980) and frog skeletal muscle (Standen, Stanfield & Ward, 1985) have an even lower unitary conductance (in the range of 15–20 pS). The channel does resemble a medium conductance channel in rat pancreatic vascular smooth muscle (Stuenkel, 1989), which shows rapid gating behaviour remarkably similar to that described in this paper.

The kinetics of the outward rectifying potassium channel was described by a model consisting of a 'fast' and a 'slow' closed state, and an open state:

$$C_f \leftrightharpoons O \leftrightharpoons C_s.$$

This is the simplest possible model given the observations that the open and closed time distributions showed a single and a double exponential decay, respectively. It was observed that the transition rate between the open and the interburst closed state was most sensitive to transmembrane potential. Under equimolar K^+ conditions a reduced voltage dependency of gating was represented as levelling of three of the four *r–V* curves. These alterations in channel properties suggest that caution must be taken in the widely used practice of characterization of potassium channels under equimolar K^+ conditions.

Barium ions had no effect on single channel conductance, but changed relatively specific the rate of open to slow closed state transitions. This effectively resulted in an increase in interburst closed periods and shortening of the burst time. A similar effect of barium ions was shown on the rat skeletal $I_{K,Ca}$ channel reconstituted in lipid bilayers (Miller, Latorre & Reisin, 1987). In this preparation initial first order gating kinetics (one open and one closed state) were modified by Ba^{2+} to the model

$$C \leftrightharpoons O \leftrightharpoons O_b \leftrightharpoons C_b$$

wherein O_b and C_b represent states where the channel is 'plugged' by barium ions. The $O–O_b$ transition rate, analogue to the $O–C_s$ transition rate in our model, is Ba^{2+} dependent, effectively introducing burst-type gating. These results show that the applied model can be an aid in pin-pointing alterations in channel behaviour caused by different modulatory factors. The model might be refined by incorporating data

such as channel regulation by intracellular metabolites, connecting the channel to signal transduction pathways.

In summary, this paper describes the outward rectifying potassium current in mouse small intestine, as studied in dispersed cells and also with an explant culturing technique that allows patch clamping on smooth muscle cells that have not been exposed to dissociation enzymes. It was shown that the potassium current is carried by a 186 pS bursting channel, of which the behaviour can be described by a three states, four transition rates model. One of the four, the open to interburst-closed transition rate, seems most sensitive to channel blockade by Ba^{2+} ions and changes in extracellular ionic composition.

The authors wish to thank Jon Lee and Laura Farraway for their collaboration. This work was supported by the Medical Research Council of Canada.

REFERENCES

ASHCROFT, F. M. (1988). Adenosine 5′-triphosphate-sensitive potassium channels. *Annual Review of Neuroscience* **11**, 97–118.

BARRY, P. H. & LYNCH, J. W. (1991). Liquid junction potentials and small cell effects in patch clamp analysis. *Journal of Membrane Biology* **121**, 101–117.

BEECH, D. J. & BOLTON, T. B. (1989). Two components of potassium current activated by depolarization of single smooth muscle cells from the rabbit portal vein. *Journal of Physiology* **418**, 293–309.

BENHAM, C. D. & BOLTON, T. B. (1983). Patch-clamp studies of slow potential-sensitive potassium channels in longitudinal smooth muscle cells of rabbit jejunum. *Journal of Physiology* **340**, 469–486.

BKAILY, G., CAILLE, J.-P., PAYET, M. D. & PEYROW, M. (1988). Bethanidine increases one type of potassium current and relaxes aortic muscle. *Canadian Journal of Physiology and Pharmacology* **66**, 731–736.

CHAMLEY CAMPBELL, J., CAMPBELL, G. R. & ROSS, R. (1979). The smooth muscle cell in culture. *Physiological Review* **59**, 1–61.

COLE, W. C. & SANDERS, K. M. (1989). Characterization of macroscopic outward currents of canine colonic myocytes. *American Journal of Physiology* **257**, C461–469.

COLQUHOUN, D. & SIGWORTH, F. J. (1983). Fitting and statistical analysis of single-channel records. In *Single Channel Recording*, ed. SAKMANN, B. & NEHER, E., pp. 191–263. Plenum Press: NY, USA.

CONTI, F. & NEHER, E. (1980). Single channel recordings of K^+ currents in squid axons. *Nature* **285**, 140–143.

FABIATO, A. & FABIATO, F. (1979). Calculator programs for computing the composition of the solutions containing multiple metals and ligands used for experiments in skinned muscle cells. *Journal de Physiologie* **75**, 463–505.

GARCIA DIAZ, J. F. (1991). Whole-cell and single channel K^+ and Cl^- currents in epithelial cells of frog skin. *Journal of General Physiology* **98**, 131–161.

HILLE, B. (1992). *Ionic Channels of Excitable Membranes*. Sinauer Associates Inc.: Sunderland, MA, USA.

LATORRE, R., OBERHAUSER, A., LABARCA, P. & ALVAREZ, O. (1989). Varieties of calcium-activated potassium channels. *Annual Review of Physiology* **51**, 385–399.

LYNCH, C. (1985). Ionic conductances in frog short skeletal muscle fibres with slow delayed rectifier currents. *Journal of Physiology* **368**, 359–378.

MILLER, C., LATORRE, R. & REISIN, I. (1987). Coupling of voltage-dependent gating and Ba^{++} block in the high-conductance, Ca^{++}-activated K^+ channel. *Journal of General Physiology* **90**, 427–449.

MOLLEMAN, A., NELEMANS, A. & DEN HERTOG, A. (1989). P_2-purinoceptor-mediated membrane currents in DDT_1 MF-2 smooth muscle cells. *European Journal of Pharmacology* **169**, 167–174.

MOLLEMAN, A., NELEMANS, A., VAN DEN AKKER, J., DUIN, M. & DEN HERTOG, A. (1991). Voltage-dependent sodium and potassium, but no calcium conductances in DDT_1 MF-2 smooth muscle cells. *Pflügers Archiv* **417**, 479–484.

NELSON, M. T., PATLAK, J. B., WORLEY, J. F. & STANDEN, N. B. (1990). Calcium channels, potassium channels, and voltage dependence of arterial smooth muscle tone. *American Journal of Physiology* **259**, C3–18.

OKABE, K., KITAMURA, K. & KURIYAMA, H. (1987). Features of 4-aminopyridine sensitive outward current observed in single smooth muscle cells from the rabbit pulmonary artery. *Pflügers Archiv* **409**, 561–568.

RUDY, B. (1988). Diversity and ubiquity of K^+ channels. *Neuroscience* **25**, 729–749.

STANDEN, N. B., STANFIELD, P. R. & WARD, T. A. (1985). Properties of single potassium channels in vesicles formed from the sarcolemma of frog skeletal muscle. *Journal of Physiology* **364**, 339–358.

STUENKEL, E. L. (1989). Single potassium channels recorded from vascular smooth muscle cells. *American Journal of Physiology* **257**, H760–769.

TAGAMI, M., NARA, Y., KUBOTA, A., SUNAGA, T., MAEZAWA, H., FUJINO, H. & YAMORI, Y. (1986). Morphological and functional differentiation of cultured vascular smooth-muscle cells. *Cell Tissue Research* **245**, 261–266.

TERADA, K., KITAMURA, K. & KURIYAMA, H. (1987). Different inhibitions of the voltage-dependent K^+ current by Ca^{2+} antagonists in the smooth muscle cell membrane of rabbit small intestine. *Pflügers Archiv* **408**, 558–564.

VOLK, K. A., MATSUDA, J. J. & SHIBATA, E. F. (1991). A voltage-dependent potassium current in rabbit coronary artery smooth muscle cells. *Journal of Physiology* **439**, 751–768.

WALSH, J. V. JR & SINGER, J. J. (1987). Identification and characterization of major ionic currents in isolated smooth muscle cells using the voltage-clamp technique. *Pflügers Archiv* **408**, 83–97.